J Antimicrob Chemother 2023; **78**: 1433–1443
https://doi.org/10.1093/jac/dkad103 Advance Access publication 12 April 2023

Journal of Antimicrobial Chemotherapy

Population pharmacokinetic modelling to characterize the effect of chronic kidney disease on tenofovir exposure after tenofovir alafenamide administration

Paul Thoueille [1], Susana Alves Saldanha[1], Vincent Desfontaine[1], Katharina Kusejko [2,3], Perrine Courlet [1], Pascal Andre[1], Matthias Cavassini [4], Laurent A. Decosterd [1], Thierry Buclin [1], Monia Guidi [1,5,6]* and the Swiss HIV Cohort Study

[1]Service and Laboratory of Clinical Pharmacology, Department of Laboratory Medicine and Pathology, Lausanne University Hospital and University of Lausanne, Lausanne, Switzerland; [2]Division of Infectious Diseases and Hospital Epidemiology, University Hospital Zurich, Zurich, Switzerland; [3]Institute of Medical Virology, University of Zurich, Zurich, Switzerland; [4]Service of Infectious Diseases, Department of Medicine, Lausanne University Hospital and University of Lausanne, Lausanne, Switzerland; [5]Centre for Research and Innovation in Clinical Pharmaceutical Sciences, Lausanne University Hospital and University of Lausanne, Lausanne, Switzerland; [6]Institute of Pharmaceutical Sciences of Western Switzerland, University of Geneva, University of Lausanne, Geneva, Switzerland

*Corresponding author. E-mail: Monia.Guidi@chuv.ch

Received 16 August 2022; accepted 17 March 2023

Background: Tenofovir alafenamide is gradually replacing tenofovir disoproxil fumarate, both prodrugs of tenofovir, in HIV prevention and treatment. There is thus an interest in describing tenofovir pharmacokinetics (PK) and its variability in people living with HIV (PLWH) under tenofovir alafenamide in a real-life setting.

Objectives: To characterize the usual range of tenofovir exposure in PLWH receiving tenofovir alafenamide, while assessing the impact of chronic kidney disease (CKD).

Methods: We conducted a population PK analysis (NONMEM®) on 877 tenofovir and 100 tenofovir alafenamide concentrations measured in 569 PLWH. Model-based simulations allowed prediction of tenofovir trough concentrations (C_{min}) in patients having various levels of renal function.

Results: Tenofovir PK was best described using a one-compartment model with linear absorption and elimination. Creatinine clearance (CL_{CR}, estimated according to Cockcroft and Gault), age, ethnicity and potent P-glycoprotein inhibitors were statistically significantly associated with tenofovir clearance. However, only CL_{CR} appeared clinically relevant. Model-based simulations revealed 294% and 515% increases of median tenofovir C_{min} in patients with CL_{CR} of 15–29 mL/min (CKD stage 3), and less than 15 mL/min (stage 4), respectively, compared with normal renal function (CL_{CR}=90–149 mL/min). Conversely, patients with augmented renal function (CL_{CR}>149 mL/min) had a 36% decrease of median tenofovir C_{min}.

Conclusions: Kidney function markedly affects circulating tenofovir exposure after tenofovir alafenamide administration in PLWH. However, considering its rapid uptake into target cells, we suggest only a cautious increase of tenofovir alafenamide dosage intervals to 2 or 3 days only in case of moderate or severe CKD, respectively.

Background

Tenofovir is an NRTI active in preventing and treating HIV-1 infection, and treating hepatitis B virus infection. It is commercially available as two prodrugs, tenofovir disoproxil fumarate and tenofovir alafenamide. Tenofovir alafenamide was developed more recently and appears to be 10 times more potent than tenofovir disoproxil fumarate, as an indirect consequence of an enhanced stability in plasma provided by the presence of a phenol and an alanine isopropyl ester. Unlike tenofovir disoproxil fumarate, which readily releases free tenofovir in the circulation, tenofovir alafenamide is taken up directly into PBMCs, where it is hydrolysed to tenofovir by intracellular cathepsin A, and then phosphorylated to produce intracellular diphosphate, the

© The Author(s) 2023. Published by Oxford University Press on behalf of British Society for Antimicrobial Chemotherapy.
This is an Open Access article distributed under the terms of the Creative Commons Attribution-NonCommercial License (https://creativecommons.org/licenses/by-nc/4.0/), which permits non-commercial re-use, distribution, and reproduction in any medium, provided the original work is properly cited. For commercial re-use, please contact journals.permissions@oup.com

Downloaded from https://academic.oup.com/jac/article/78/6/1433/7115733 by Université de Lausanne user on 17 January 2024

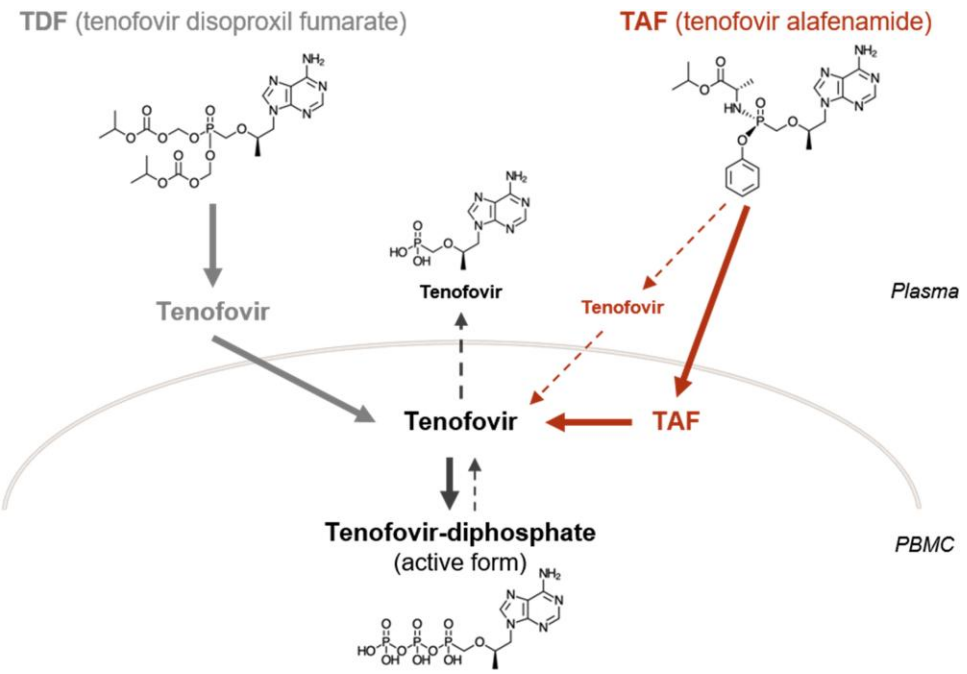

Figure 1. Comparison of HIV-target cell loading mechanisms by tenofovir disoproxil fumarate (TDF) and tenofovir alafenamide (TAF). Bold arrows illustrate major routes, whereas dashed arrows illustrate minor routes. This figure appears in colour in the online version of *JAC* and in black and white in the print version of *JAC*.

molecule active against HIV reverse transcriptase (Figure 1).[1,2] This preferential uptake by PBMCs results in significantly higher intracellular levels of tenofovir diphosphate despite 90% lower plasma levels of tenofovir observed under standard tenofovir alafenamide versus tenofovir disoproxil fumarate dosage.[3–5] Because plasma levels of tenofovir are associated with kidney tubular damage and, in the long term, bone demineralization, this systemic toxicity is significantly reduced with tenofovir alafenamide.[1,6]

In HIV-1 treatment, tenofovir alafenamide is administered orally at the standard dosage of 25 mg q24h, or 10 mg q24h when coadministered with a booster such as cobicistat, able to increase tenofovir alafenamide exposure by inhibiting intestinal P-glycoprotein (P-gp).[7–9] Significant interactions with cytochromes P450 are not reported. However, because tenofovir alafenamide is a substrate of P-gp, breast cancer resistance protein (BCRP) and organic anion transporting polypeptides (OATPs), potent P-gp, BCRP and/or OATP inducers or inhibitors may lead to under- or overexposure, respectively, with potential HIV-1 treatment failure or increased toxicity. In addition, due to kidney elimination of tenofovir by both glomerular filtration and active tubular secretion, renal diseases or comedication with nephrotoxic drugs may increase the plasma concentrations of tenofovir.[2,10,11] No dosage adjustment of tenofovir alafenamide is currently recommended as long as creatinine clearance (CL_{CR}) exceeds 30 mL/min, nor in patients receiving haemodialysis.[12]

Even if not universally recommended as first-line treatment,[13] tenofovir alafenamide is progressively preferred to tenofovir disoproxil fumarate due to its better tolerability, and is now proposed as a component of first-line antiretroviral combinations for HIV treatment.[14] Yet, although population pharmacokinetic (popPK) studies of tenofovir alafenamide have been published,[15–17] there is, to the best of our knowledge, no popPK analysis of tenofovir after tenofovir alafenamide administration assessing the impact of chronic kidney disease (CKD) on tenofovir plasma exposure. Clearly, monitoring intracellular levels (i.e. tenofovir diphosphate) would correlate more reliably with clinical response. However, PBMC assays require more infrastructure and resources than standard blood samples,[18,19] which hinders their clinical implementation. The characterization of the concentration–time profile of tenofovir and its associated variability in people living with HIV (PLWH) under tenofovir alafenamide in a real-life setting is therefore relevant because of the availability of therapeutic drug monitoring (TDM) for tenofovir.[20,21] Bayesian calculations based on real-life popPK data would then help to establish reference percentile curves, facilitating the interpretation of drug concentration measurements as part of a clinical TDM programme, as offered in our institution among others.

Methods

Study population

This study is an extension of project #815 of the Swiss HIV Cohort Study (SHCS; http://www.shcs.ch), which aimed to assess clinically significant drug–drug interactions between antiretrovirals and frequently prescribed comedications.[22]

Plasma samples were obtained from patients enrolled in the SHCS#815 project and receiving tenofovir as tenofovir alafenamide on a daily basis (either 25 mg or 10 mg plus cobicistat). The analysis was complemented with anonymized data obtained from SHCS patients followed in the routine TDM programme of the Service of Clinical Pharmacology in Lausanne (Switzerland) between January 2017 and

Downloaded from https://academic.oup.com/jac/article/78/6/1433/7115733 by Université de Lausanne user on 17 January 2024

Table 1. Characteristics of the PLWH enrolled in the study for population PK model development and validation

	Model-building dataset ($n=486$)		Validation dataset ($n=83$)	
Baseline characteristic	Value	% or range	Value	% or range
Demographic characteristics				
Sex (no.):				
Male	339	70	48	58
Female	147	30	28	34
Unknown	—	—	7	8
Ethnicity (no.):				
White	347	71	45	54
Black	109	23	23	28
Hispanic American	19	4	5	6
Asian	11	2	1	1
Other	—	—	1	1
Unknown	—	—	8	10
Median age (years)	51	19–79	53	29–76
Median body weight (kg)	74	42–142	72	37–103
Median height (cm)	173	145–195	172	151–194
Median BMI (kg/m^2)	24	15–51	25	13–38
Physiological characteristics				
Serum creatinine (μmol/L)	85	42–256	88	51–136
CL_{CR} (mL/min)[a]	93	33–203	88	38–167
eGFR (mL/min/1.73 m^2)[b]	87	23–153	83	46–134
Antiretroviral therapy[c]				
Bictegravir	85	17	29	35
Cobicistat	277	43	22	27
Darunavir	34	7	7	8
Dolutegravir	50	10	6	7
Doravirine	3	0.5	8	10
Elvitegravir	141	29	7	8
Emtricitabine	403	83	51	61
Raltegravir	10	2	1	1
Rilpivirine	16	3	4	5
Co-administered drugs[d]				
Potent P-gp inhibitors	45	9	9	11
Moderate P-gp inhibitors	9	2	1	1
P-gp inducers	4	1	—	—
OATP (1B1 or 1B3) inhibitors	14	3	2	2
Nephrotoxic drugs	47	10	6	7

CL_{CR}, creatinine clearance; eGFR, estimated glomerular filtration rate; OATP, organic-anion-transporting polypeptides; P-gp, P-glycoprotein.
[a]CL_{CR} calculated according to the Cockcroft and Gault equation.[27]
[b]eGFR calculated according to the equations reported by Levey *et al.* (CKD-EPI).[28]
[c]Principal HIV medications retrieved from the SHCS database. Cobicistat is co-administered with 10 mg dose of tenofovir alafenamide.
[d]Potent P-gp inhibitors (amiodarone, carvedilol, clarithromycin, fluoxetine, itraconazole, methadone, quetiapine, rilpivirine, risperidone, ritonavir and sertraline), moderate P-gp inhibitors (atazanavir, diltiazem, duloxetine and efavirenz), P-gp inducers (rifabutine, nevirapine), OATP inhibitors (atazanavir, clarithromycin, ritonavir)[29–32] and nephrotoxic drugs (antihypertensive drugs: candesartan, captopril, hydrochlorothiazide, lisinopril, olmesartan, valsartan; antiviral: aciclovir, valaciclovir, valganciclovir; immunosuppressor: tacrolimus; NSAIDs: acetylsalicylic acid, ibuprofen, naproxen)[33–35] retrieved from the SHCS database.

January 2021. The sparse samples obtained from SHCS#815 project and the routine TDM programme were supplemented with detailed sampling data. The detailed sampling plan in SHCS#815 included blood sampling right before dose intake and then at 0.5, 1, 2, 3, 4, 6, 8, 10, 12 and 24 h (trough level) post dose. Exclusion criteria were undetectable tenofovir plasma concentration, considered specific for absolute non-adherence to treatment, and non-reliable information on time and/or date of last drug intake and/or blood collection. Demographic factors, clinical information and comedications were recorded during the routine SHCS visits (every 3–6 months).

Downloaded from https://academic.oup.com/jac/article/78/6/1433/7115733 by Université de Lausanne user on 17 January 2024

Notably, because of the very short half-life of tenofovir alafenamide in plasma (i.e. 0.5 h),[23] only samples with a reported time after administration of less than 6 h were selected for the determination of tenofovir alafenamide concentration in plasma, resulting in 100 samples analysed.

Analytical method

The MS assay used for the analysis of plasma samples was adapted from a previously published validated multiplex method (details are provided in Supplementary Methods, available as Supplementary data at *JAC* Online).[20] The limit of quantification of the method was 1 ng/mL for both tenofovir and tenofovir alafenamide.

PopPK analysis

The non-linear mixed effects modelling software NONMEM® (v7.4.3, ICON Development Solutions, Ellicott City, MD, USA), assisted by PsN v4.8.0[24] and Pirana v2.9.2,[25] was used for popPK analyses. Data management, graphical exploration and statistical analyses were performed with R (v4.0.2; R Development Core Team, http://www.r-project.org/).

The popPK analyses were performed converting tenofovir alafenamide doses into nanomoles, and the measured concentrations of tenofovir alafenamide and tenofovir into nanomoles per millilitre. Steady state was assumed in all individuals. The data were split into model development and validation datasets, with patients having complete information, including tenofovir alafenamide concentration measurements, assigned to the first one with priority. Subsequently, the remaining data were randomly assigned to one or the other data set.

Structural model

A stepwise procedure allowed identifying the models that best fit tenofovir alafenamide and tenofovir simultaneously (ADVAN 5 in NONMEM), and then exclusively tenofovir data (ADVAN2), by comparing various compartmental models with linear elimination and absorption processes. Because of the small number of samples collected right after drug intake, the first-order absorption rate (k_{12}) of tenofovir alafenamide could not be correctly estimated and was thus fixed to 2 h^{-1} based on early model development (i.e. preliminary tests on our data), and in accordance with published values.[12,26] During the subsequent analysis neglecting tenofovir alafenamide concentrations, the first-order absorption rate of tenofovir (k_a) was also fixed to 2 h^{-1} owing to the flip-flop kinetics that appears to characterize tenofovir alafenamide disposition.[16] The coadministration of cobicistat was forced as covariate into the model to estimate the relative bioavailability (F) of tenofovir alafenamide administered daily at 10 mg with cobicistat compared with 25 mg alone ($F=1$) to account for dose variation. Because tenofovir alafenamide is rapidly and almost completely metabolized into tenofovir, a complete and irreversible conversion of tenofovir alafenamide into tenofovir was assumed. Parametrization was performed in terms of apparent clearances (CL_{TAF} for tenofovir alafenamide and CL_{TFV} for tenofovir) and volumes of distribution (V_{TAF} for tenofovir alafenamide and V_{TFV} for tenofovir), in addition to F and k_{12} or k_a. All the parameters were assumed to follow a log-normal distribution, and between-subject variability (BSV) was sequentially tested for all of them. Because tenofovir alafenamide is only administered orally, all clearance and volume estimates represent apparent values (i.e. relative to F). Finally, proportional, additive and mixed error models were compared to evaluate tenofovir alafenamide and tenofovir residual unexplained variability (RUV), with distinct RUVs per compound and a correlation term (i.e. L2 item in NONMEM®) evaluated when tenofovir alafenamide and tenofovir were modelled simultaneously.

Covariate model

Available covariates were age, sex, ethnicity, bodyweight, height, BMI, serum creatinine, CL_{CR} (calculated by the Cockcroft and Gault equation[27]), estimated glomerular filtration rate (eGFR, CKD-EPI equation[28]) and co-medications. The concomitant drugs covariate analysis focused on potent P-gp inhibitors, moderate P-gp inhibitors, P-gp inducers and OATP inhibitors[29–32] found in patients' treatment (Table 1). Of note and as previously explained, cobicistat was not included in the analysis of P-gp inhibitors. However, a 'ceiling effect' due to cobicistat inhibition, which would result in a reduced magnitude of the effect of P-gp inhibitors, was investigated comparing patients receiving cobicistat or not. Nephrotoxic drugs[33–35] identified in the patient's record (Table 1) were not tested, because their impact was considered as taken into account by the biomarkers of kidney failure (i.e. CL_{CR} and eGFR). Correlations between individual PK parameter estimates and biologically plausible covariates were first explored graphically to identify possible relationships. A stepwise forward insertion/backward deletion approach was then conducted to identify statistically significant covariates using appropriate linear or non-linear functions. Ethnicity was first modelled assigning a separate PK parameter per group (rich model), and then per regrouped ethnicities (reduced model). Lastly, the statistically significant parameters were combined in a multivariate approach to build up an intermediate model, from which backward deletion was applied for final model identification.

Model selection and parameter estimation

Tenofovir and tenofovir alafenamide data were fitted using a first-order conditional estimation method with interaction, with a Laplacian option when the M3 method was tested to handle tenofovir alafenamide BQL data. These data were alternatively modelled with the M6 approach.[36]

Variation of the NONMEM® objective function value (ΔOFV) allowed discriminating between hierarchical models ($P=0.05$ and $P=0.01$ for forward and backward steps, respectively), whereas Akaike's information criterion was used for non-nested models. In addition to statistical criteria, the final covariate model was chosen according to the principle of parsimony,[37] clinical considerations, and the quantification of BSV explained by the introduction of covariates, which brings valuable information for assessing the importance of covariates on the dependent outcomes.[38,39] Finally, the precision of PK parameter estimates and model shrinkages, as well as diagnostic plots, helped model selection and assessment of results reliability.

Model evaluation and assessment

Prediction- and variability-corrected visual predictive checks (pvcVPCs) were performed on the final PK models to compare the observed concentrations with the 5th, 50th and 95th prediction percentiles.[24,40,41] In addition, the bootstrap method ($n=2000$) assisted model evaluation by comparing the original model estimates with the bootstrap median parameter values and their 95% CIs. The external validation of the tenofovir model alone was performed using the validation dataset and comparing log-transformed concentrations and predictions with mean prediction error (MPE) and root mean square error, which quantify final model accuracy and precision, respectively.[42]

Model-based simulations

Simulations were performed to assess the clinical significance of all the covariates by simulating 1000 individuals in each group with the factor of interest (or a combination of factors) to derive the corresponding tenofovir and tenofovir alafenamide PK profiles and AUC, as well as the median tenofovir trough concentration (C_{min}). In particular, the impact of kidney function on tenofovir exposure was evaluated by simulating 1000 individuals with different CKD stages (i.e. augmented kidney function: 200–150 mL/min; normal kidney function: 90–149 mL/min; stage 1: 60–89 mL/min; stage 2: 30–59 mL/min; stage 3: 15–29 mL/min; stage 4: <15 mL/min) using a reduced model containing only CL_{CR} as covariate.

Downloaded from https://academic.oup.com/jac/article/78/6/1433/7115733 by Université de Lausanne user on 17 January 2024

Uniform distributions of CL_{CR} were assumed to generate individual renal function values in each range.

Results

Overall, 569 PLWH contributed to 877 tenofovir and 100 tenofovir alafenamide concentrations (Figure S1). A total of 793 tenofovir (44 from four patients undergoing detailed PK sampling), and 100 tenofovir alafenamide (15 non-BQL concentrations from detailed PK sampling) concentrations, collected in 486 PLWH, were available for the development of popPK models. The external validation of the tenofovir model alone was carried out on 84 data of 83 PLWH. None of the tenofovir concentrations were BQL but 47 tenofovir alafenamide were. Apart from the patients of the SHCS #815 undergoing detailed PK sampling, one to two samples per patient were available. Table 1 summarizes the characteristics of the study population, whereas Table S1 shows the characteristics of the reduced dataset of PLWH with tenofovir alafenamide measurements.

Structural, statistical and covariate models

A one compartment model with first order-absorption and elimination through complete conversion into tenofovir for tenofovir alafenamide, and an additional compartment with linear elimination for tenofovir best captured joint tenofovir alafenamide and tenofovir disposition (Figure 2, upper panel). This model, detailed in Supplementary Methods, showed that tenofovir alafenamide is characterized by 'flip-flop' kinetics (i.e. k_{12} < elimination rate constant k_{23}), indicating almost instantaneous tenofovir alafenamide conversion into tenofovir. Consequently, it provided exactly the same description and parameter values for tenofovir as the model developed from the tenofovir data alone. Because only tenofovir is quantified in routine clinical practice, and because of the small number of tenofovir alafenamide concentrations available, this section focuses on the description of tenofovir alone analysis. These data were best described by a one-compartment model with linear absorption and elimination (Figure 2, lower panel). The assignment of BSV on F significantly improved data description ($\Delta OFV = -16$, $P < 0.001$), but no further changes were observed when adding BSV on k_a, CL_{TFV} or V_{TFV} ($\Delta OFV > -1$). An additive error model best described tenofovir RUV. Base model parameter estimates were a V_{TFV} of 2660 L and a CL_{TFV} of 39.9 L/h, while fixing k_a to 2 h^{-1} and F to 1 for patients under tenofovir alafenamide 25 mg with a BSV of 34%. In addition, cobicistat increased F by 115%, consistent with the recommendation of reducing tenofovir alafenamide dose to 10 mg in case of co-administration with cobicistat. Univariate analyses revealed clear effects of CL_{CR} ($\Delta OFV = -285$, $P < 0.001$), eGFR ($\Delta OFV = -242$, $P < 0.001$), age ($\Delta OFV = -150$, $P < 0.001$), ethnicity (full covariate model $\Delta OFV = -37$, $P < 0.001$), bodyweight ($\Delta OFV = -15$, $P < 0.001$) and co-administration of potent P-gp inhibitors ($\Delta OFV = -11$, $P < 0.001$) on CL_{TFV}. A reduced covariate model with White and Asian patients, set as the reference group, versus Black and Hispanic American patients was used for ethnicity ($\Delta OFV = +2$, compared with the full covariate model, $P > 0.05$). After backward deletion and application of the principle of parsimony,[37] a full model incorporating the effect of CL_{CR}, age, ethnicity and potent P-gp inhibitors on CL_{TFV} was retained. The results showed that Black and Hispano American patients had a 12% increased CL_{TFV} compared with White and Asian patients, and that co-administration of potent P-gp inhibitors (namely carvedilol and sertraline) reduced CL_{TFV} by 12%, independently of the presence of cobicistat. In addition, individuals with a CL_{CR} of 20 mL/min (stage 3 CKD) would have a CL_{TFV} of 18 L/h, which is 57% lower than the CL_{TFV} of 42 L/h obtained for those with normal kidney function. On the other hand, 80-year-olds, for example, would have a CL_{TFV} reduced to 36 L/h compared with younger PLWH (i.e. median age 51 years, CL_{TFV} of 42 L/h).

The covariates included in the full popPK model explained altogether 59% of the BSV on F, with 53% resulting from the inclusion of CL_{CR} alone. Retaining only the effect of CL_{CR} on CL_{TFV} (reduced model) would thus be appropriate for a model aimed at supporting TDM in routine clinical care. Table 2 and Table S2 present the parameter estimates with their bootstrap evaluations of the full and reduced popPK models, respectively, and Figure S2 shows the diagnostic plots of the latter. Population parameter estimates of tenofovir alafenamide and tenofovir with their bootstrap evaluations, and diagnostic plots, are presented in Table S3 and Figure S3, respectively.

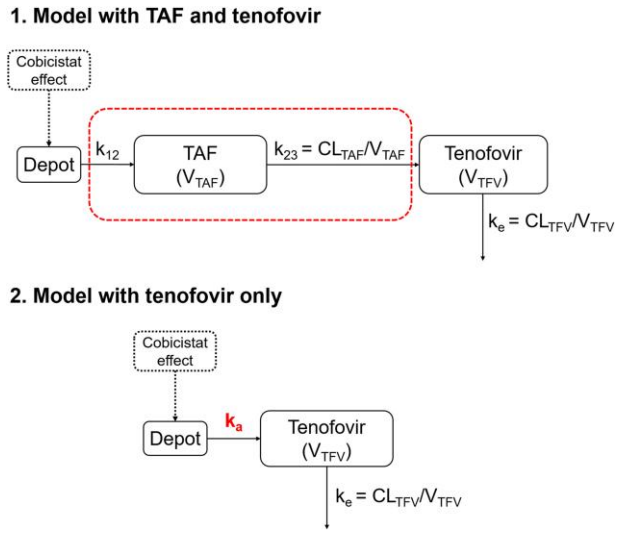

Figure 2. Compartmental models used to describe simultaneously tenofovir and tenofovir alafenamide (TAF) (Model 1) and tenofovir alone (Model 2) concentration–time profiles. CL_{TAF}, apparent clearance of TAF; CL_{TFV}, apparent clearance of tenofovir; k_a, first-order absorption rate constant of tenofovir; k_e, tenofovir elimination rate constant; k_{12}, absorption rate constant from depot to the TAF compartment; k_{23}, rate constant from TAF compartment to the tenofovir compartment; V_{TAF}, apparent volume of distribution of TAF; V_{TFV}, apparent volume of distribution of tenofovir. This figure appears in colour in the online version of *JAC* and in black and white in the print version of *JAC*.

Model evaluation

The bootstrap results demonstrate reliability of both full final and reduced models, and the pvcVPCs (Figure 3) confirm their good performance (see Figure S4 for the model incorporating tenofovir alafenamide and tenofovir). Lastly, a similar non-significant bias (MPE = 3.6%, 95% CI = 0.2%–7.1%) with a precision of 17% was

Downloaded from https://academic.oup.com/jac/article/78/6/1433/7115733 by Université de Lausanne user on 17 January 2024

Table 2. Final population PK parameter estimates of tenofovir with their bootstrap evaluations

	Final model				Bootstrap (n = 2000 samples)			
Parameters	Estimate	RSE (%)[a]	BSV (%)	RSE (%)[a]	Median	95% CI	BSV (%)	95% CI
k_a (h^{-1})	2 FIX	—			2 FIX	—		
V_{TFV} (L)	2390	9			2397	2037–2891		
CL_{TFV} (L/h)	42.2	2			42.3	40.1–44.3		
θ_{CLCR}	0.707	10			0.703	0.549–0.837		
θ_{Age}	−0.244	30			−0.242	−0.398 to −0.099		
$\theta_{Black\ or\ Hispano\ American}$	0.119	23			0.120	0.068–0.175		
$\theta_{Potent\ P\text{-}gp\ inhibitors}$	−0.121	39			−0.119	−0.202 to 0		
F (%)	1 FIX	—	21.1	6	1 FIX	—	20.9	18.4–23.5
$\theta_{Cobicistat}$	1.15	6			1.16	1.02–1.28		
σ_{add} (nmol/mL)	0.0099	5			0.0099	0.0088–0.0110		

Final model:

$$TVCL_{TFV} = CL_{TFV} \times \left(1 + \theta_{CLCR} \times \frac{(CL_{CR} - CL_{CR-ref})}{CL_{CR-ref}}\right) \times \left(1 + \theta_{Age} \times \frac{(Age - Age_{median})}{Age_{median}}\right) \times (1 + \theta_{Black\ or\ Hispano\ American}) \times (1 + \theta_{Potent\ P-gp\ inhibitors})$$

$$TVF = 1 + \theta_{Cobicistat}$$

BSV, between-subject variability; CL_{CR}, creatinine clearance; CL_{TFV}, apparent clearance of tenofovir; F, relative bioavailability; k_a, first-order absorption rate constant; RSE, relative standard error; $TVCL_{TFV}$, typical value of CL_{TFV}; TVF, typical value of F; V_{TFV}, apparent volume of distribution of tenofovir; θ_{CLCR}, creatinine clearance (CL_{CR}) effect on CL_{TFV} and $CL_{CR\text{-}ref}$ = 100 mL/min; θ_{Age}, age effect on CL_{TFV} and Age_{median} = 51 years old, median age value in the study population; $\theta_{Black\ or\ Hispano\ American}$, Black or Hispano American ethnicity effect on CL_{TFV}; $\theta_{Potent\ P\text{-}gp\ inhibitors}$, potent P-gp inhibitors effect on CL_{TFV}; $\theta_{Cobicistat}$, effect of cobicistat on F; σ_{add}, additive residual error.
[a]Relative standard error (RSE) of the estimate defined as standard error (SE) of the estimate/estimate, expressed as a percentage, with SE estimate retrieved directly from the NONMEM output file.

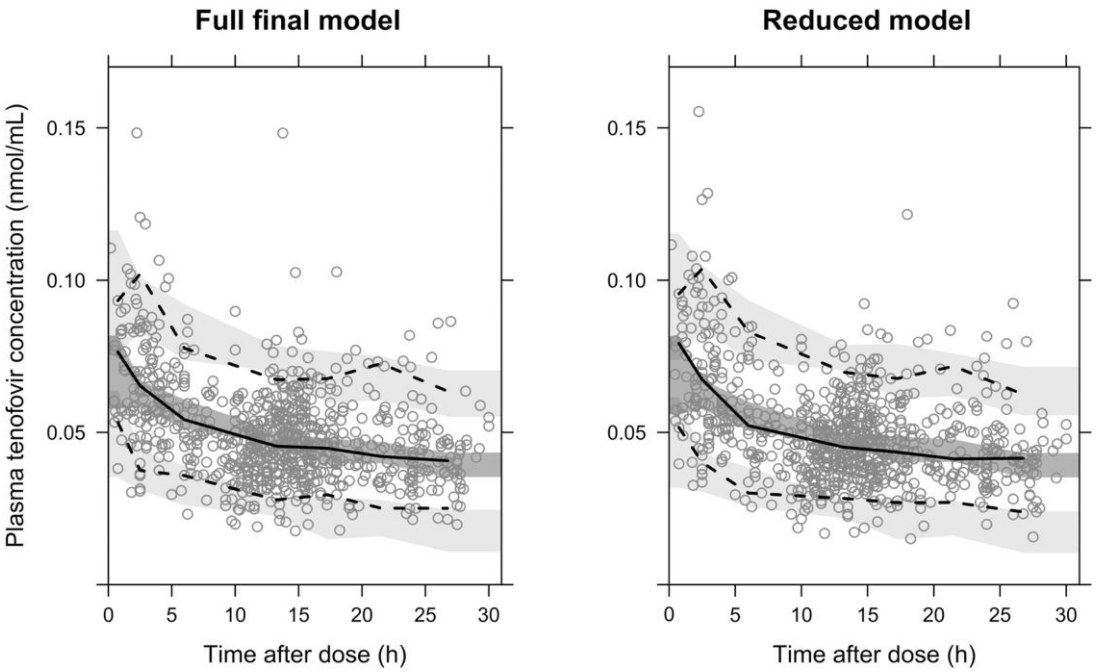

Figure 3. Visual predictive check of the full final model (left panel) and reduced model (right panel) for tenofovir. Open circles represent the observed plasma concentrations; solid and dashed lines represent the median and $PI_{90\%}$ of the observed data, respectively; shaded surfaces represent the model-predicted 90% CI of the simulated median and $PI_{90\%}$. Note: concentrations with time after dose beyond 30 h (7 out of the 790) are not displayed. $PI_{90\%}$, 90% prediction intervals.

Downloaded from https://academic.oup.com/jac/article/78/6/1433/7115733 by Université de Lausanne user on 17 January 2024

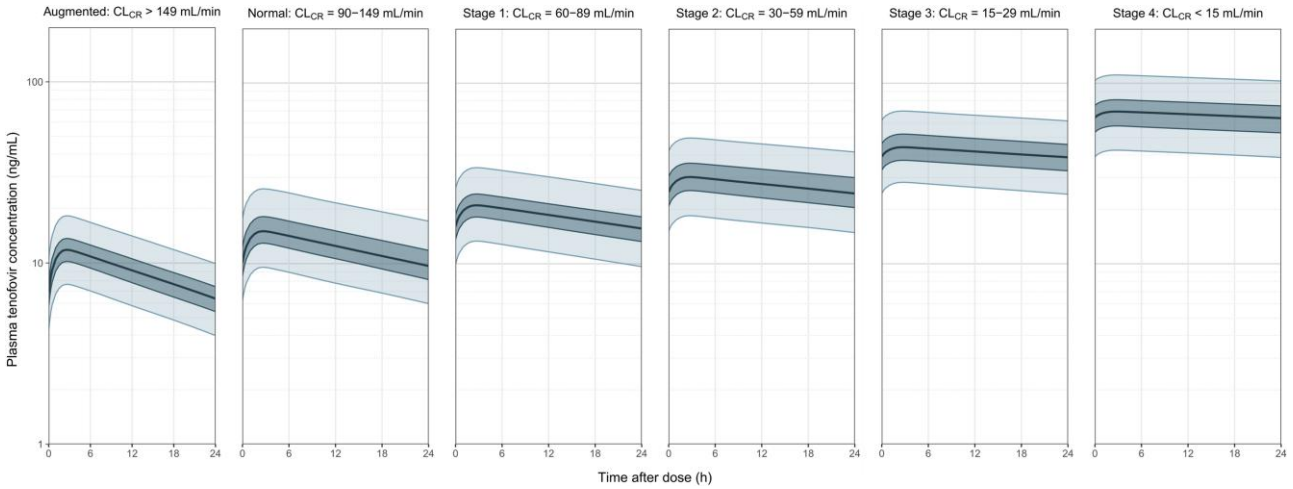

Figure 4. Simulated PK profiles for tenofovir after 25 mg tenofovir alafenamide administration in individuals with different CKD stages obtained with the reduced model. Solid lines represent the 2.5%, 25%, 50% (median), 75% and 97.5% percentiles. The dark surfaces thus encompass the corresponding 50% prediction intervals of the simulated data, and the light surfaces the 95% prediction intervals. This figure appears in colour in the online version of *JAC* and in black and white in the print version of *JAC*.

Table 3. Tenofovir model-predicted secondary PK exposure levels for the different CKD stages obtained using the reduced model

		Kidney function[a]					
Dosage	Exposure metric	Augmented	Normal	Stage 1	Stage 2	Stage 3	Stage 4
TAF	AUC_{0-24} (ng•h/mL)	218	298	444	660	1000	1610
25 mg q.d. without cobicistat		[139–337]	[187–519]	[277–720]	[402–1100]	[633–1589]	[981–2574]
	C_{min} (ng/mL)	6.4	9.7	15.7	24.5	38.9	64.1
		[4.0–9.9]	[6.0–17.2]	[9.6–25.5]	[14.9–41.6]	[24.3–61.8]	[38.8–102.9]
TAF	AUC_{0-24} (ng•h/mL)	183	257	374	555	854	1325
10 mg q.d.		[116–293]	[155–422]	[243–580]	[327–928]	[522–1368]	[783–2217]
with cobicistat	C_{min} (ng/mL)	5.3	8.3	13.2	20.7	33.1	52.7
		[3.3–8.7]	[4.9–14.2]	[8.4–20.6]	[12.0–35.2]	[20.1–53.4]	[30.9–88.9]

CL_{CR}, creatinine clearance; q.d., once daily; TAF, tenofovir alafenamide.
[a]Augmented kidney function: CL_{CR}=200–150 mL/min; normal kidney function: CL_{CR}=90–149 mL/min; stage 1: CL_{CR}=60–89 mL/min; stage 2: CL_{CR}=30–59 mL/min; stage 3: CL_{CR}=15–29 mL/min; stage 4: CL_{CR}<15 mL/min. Median derived predictions [95% prediction intervals].

observed for both the full final and the reduced models with the external validation.

Simulations

Tenofovir exposures following administration of 25 mg tenofovir alafenamide or 10 mg tenofovir alafenamide plus cobicistat were judged equivalent. No clinically relevant differences in median C_{min} between ethnic groups, or with or without the presence of potent P-gp inhibitors were predicted. In addition, the effect of age on tenofovir C_{min} within the different CKD stages was considered minor (Figure S5). These results further support the use of the reduced model to describe the impact of CKD on circulating tenofovir exposure.

The median C_{min} calculated for patients with normal kidney function using the reduced model was 9.7 ng/mL, and thus in accordance with the usual target used in routine TDM.[4,43,44] Simulations obtained with the reduced model showed 59%, 143%, 294% and 515% increases of median tenofovir C_{min} in patients with stage 1, 2, 3 and 4 CKD, respectively, compared with patients with normal kidney function. Conversely, patients with augmented kidney function had a 36% decrease of median tenofovir C_{min}. No difference was predicted regarding tenofovir alafenamide concentrations in patients with CKD compared with normal renal function. Figure 4 presents the simulated PK profiles of tenofovir for different CKD stages, and Table 3 the derived PK exposure metrics. Lastly, Figure S6 shows the simulated PK profiles for tenofovir along the concentrations measured in individuals.

Discussion

The present study describes the popPK profile of tenofovir observed among PLWH in a real-life setting, while revealing the

Downloaded from https://academic.oup.com/jac/article/78/6/1433/7115733 by Université de Lausanne user on 17 January 2024

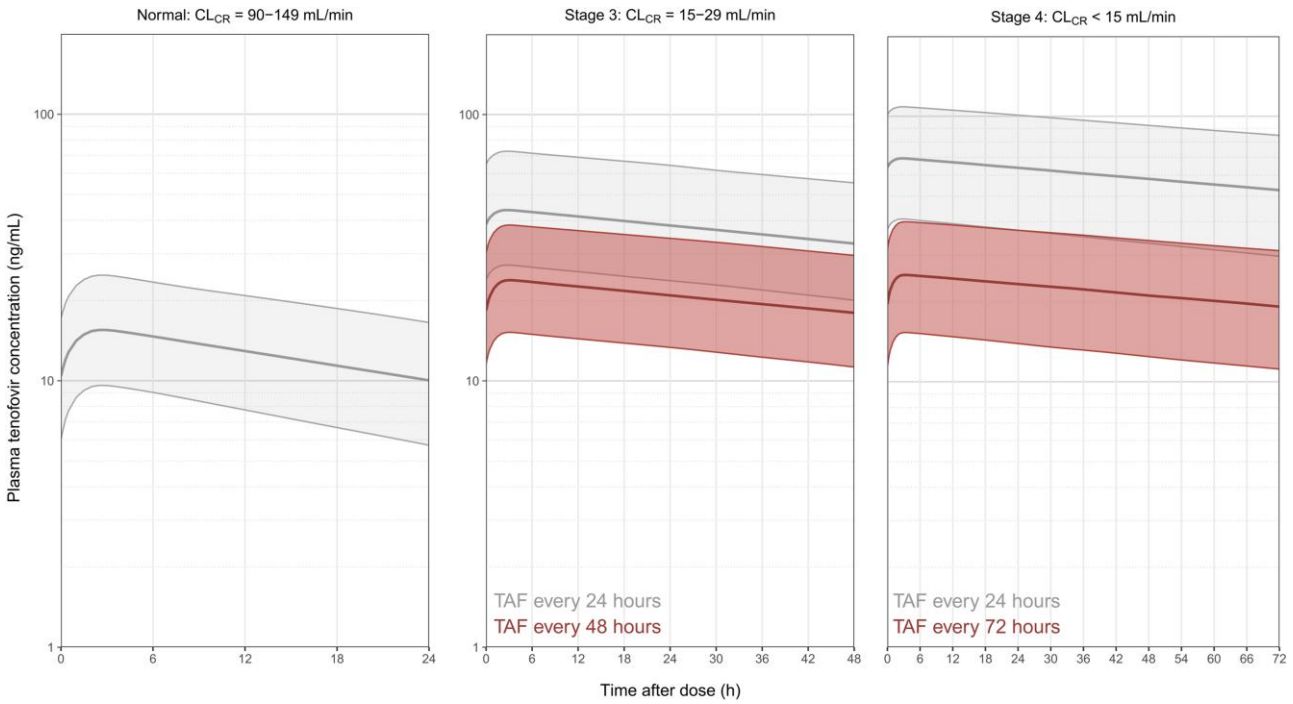

Figure 5. Simulated PK profiles for tenofovir after 25 mg tenofovir alafenamide administration in stage 3 and 4 CKD individuals, before (light-grey surfaces) and after (dark-red surfaces) the proposed dosage adjustment for stage 3 and stage 4 kidney insufficiency. The less-than-proportional adjustment results in higher plasma exposure but should ensure sufficient intracellular exposure. Solid lines represent the 2.5%, 50% (median) and 97.5% percentiles. The surfaces encompass the 95% prediction intervals of the simulated data. This figure appears in colour in the online version of *JAC* and in black and white in the print version of *JAC*.

important impact of CKD on tenofovir exposure after tenofovir alafenamide administration. The absorption process of tenofovir in the model reflects the intracellular uptake of tenofovir alafenamide and its conversion into tenofovir in the cell, and entry into the systemic circulation. Here, tenofovir displays flip-flop kinetics relative to tenofovir PK following tenofovir disoproxil fumarate dosing, implying that the combined rate of absorption, conversion and re-entry is the rate-limiting factor in tenofovir PK.[16] Cobicistat increases by 115% the absorption of tenofovir alafenamide and consequently the production of tenofovir. Because of the lack of very early tenofovir alafenamide measurements, the effect of cobicistat was incorporated into the overall bioavailability, *F*, which corrects for tenofovir alafenamide dose and also accounts for BSV on tenofovir production (i.e. the complex multistep biotransformation of tenofovir alafenamide to tenofovir). It is conceivable that BSV also affects other PK parameters such as CL and *V*. However, in the absence of intravenous data, precise discrimination of the amount of BSV affecting the different PK parameters is impossible. It is common in popPK modelling to see the main source of variability lumping together all less important BSV components affecting other parameters. Cobicistat could also differently affect tenofovir alafenamide absorption and cellular uptake, involving processes that our model could not individually capture. Indeed, because tenofovir alafenamide is a substrate of P-gp, cobicistat should theoretically affect tenofovir alafenamide entry into PBMCs by reducing tenofovir alafenamide efflux from the cells, thus increasing tenofovir production. Tenofovir T_{max} derived using the base model was 2.4 h, which corresponds to the value reported in the literature.[3,43,45] In addition, the half-life of 46 h is roughly in accordance with the value of approximately 32 h reported in the official monography, probably observed in healthy volunteers with normal renal function.[12]

Overall, the simulated tenofovir exposures for different kidney function levels are consistent with the currently available data.[12,46] Our simulations performed using the reduced model showed that patients with stage 3 or 4 CKD reach plasma tenofovir concentrations similar to those seen after tenofovir disoproxil fumarate administration in patients with normal kidney function.[3,47,48] Adjustment of the frequency of tenofovir disoproxil fumarate administration to every 48–96 h is currently recommended in patients with a CL_{CR} less than 50 mL/min.[10,49] However, tenofovir alafenamide and tenofovir disoproxil fumarate have distinct pathways to their site of action: tenofovir alafenamide is almost completely internalized into PBMCs and then converted into tenofovir diphosphate, in contrast to tenofovir disoproxil fumarate, which is predominantly hydrolysed into tenofovir in plasma prior to uptake by PBMCs and conversion into tenofovir diphosphate (Figure 1). Therefore, a similar adjustment of tenofovir alafenamide dosage according to kidney function would certainly drive plasma tenofovir concentrations close to levels observed in patients with fully functional kidneys, but may theoretically result in a lower PBMC load and therefore insufficient intracellular tenofovir diphosphate exposure. By a thorough literature review we have identified five clinical studies that compared plasma tenofovir and PBMC tenofovir diphosphate levels

Downloaded from https://academic.oup.com/jac/article/78/6/1433/7115733 by Université de Lausanne user on 17 January 2024

under tenofovir disoproxil fumarate and tenofovir alafenamide (Table S4).[4,44,50–52] On average, a standard dosage of tenofovir alafenamide produces plasma tenofovir levels representing only 15% of those observed under usual tenofovir disoproxil fumarate doses (10%–22% according to the studies under consideration), for a six-fold higher intracellular exposure in tenofovir diphosphate (2.7- to 10-fold across the studies). Considering, for example, a patient with stage 3 CKD, a literal interpretation of our model might lead to the suggestion of adjusting the dosage of tenofovir alafenamide down to one-quarter of the standard dosage, which could be conveniently achieved by giving one dose every 4 days considering the prolonged half-life of tenofovir in this condition. Even though intracellular tenofovir diphosphate exposure is expected to be reduced by the same ratio, it would still remain 50% higher than the exposure observed under conventional tenofovir disoproxil fumarate treatment, considered clinically effective (Table S4). Thus, the preferential loading of tenofovir alafenamide by PBMCs challenges the premise of a drastic dosage adjustment based on renal function. A dosage adjustment to one-half of the standard dosage is probably sufficient, because the expected circulating tenofovir levels would remain one-third of those associated with conventional tenofovir disoproxil fumarate treatment, thus having little chance to result in clinically significant toxicity. Simultaneously, twice higher circulating levels would increase the intracellular passage of plasma tenofovir. A similar logic would lead to propose an adjustment to one-third of the tenofovir alafenamide standard dosage in stage 4 CKD patients, in which our model predicts a six-fold increase of tenofovir levels. Figure 5 illustrates these recommendations for dosage adjustments. In a study addressing the consequences of incomplete therapeutic adherence, Yager *et al.*[50] reported that levels of tenofovir diphosphate were still 2.6 times higher in patients taking tenofovir alafenamide doses only once every 3 days than in patients receiving tenofovir disoproxil fumarate every day. This evidence indicates that tenofovir alafenamide is more permissive than tenofovir disoproxil fumarate with respect to missed doses or longer dosing intervals. Put simply, based on those considerations, patients with stage 3 or 4 CKD should ideally receive tenofovir alafenamide once every 2 or 3 days, respectively, in order to maintain safe circulating levels of tenofovir while preserving sufficient tenofovir diphosphate exposure in target HIV-infected cells.

Limitations of the present work should be acknowledged. Tenofovir concentrations in plasma are currently used in routine TDM as reference for treatment exposure, although the relationship between plasma and intracellular levels is at best indirect.[53,54] Because tenofovir alafenamide is rapidly and largely internalized in the target cells, monitoring of plasma tenofovir levels appears to be mainly based on the measurement of tenofovir released into the bloodstream, prior to its elimination by the kidneys. However, although it is clear that monitoring intracellular levels would probably be more reliably related to clinical response, it is more difficult to implement in clinical practice because PBMC assays demand more infrastructure and resources.[18,19] In this case, monitoring of plasma tenofovir concentration remains a surrogate for intracellular concentrations and a convenient tool available to assess treatment exposure, along with monitoring viral suppression and CD4 counts. Lastly, despite similar expected PK,[23] further studies need to be performed in patients with hepatitis B to verify whether our observations apply as well to this population.

In conclusion, our study demonstrates that CL_{CR} is the main factor affecting circulating tenofovir exposure after tenofovir alafenamide administration. Our model reveals that patients with stage 3 and stage 4 CKD reach plasma tenofovir exposure of the same order as patients with normal kidney function receiving tenofovir disoproxil fumarate. A dosage adaptation to one-half and one-third of the standard tenofovir alafenamide regimen seems reasonable in patients with stage 3 and 4 CKD, respectively. A prospective validation of these suggestions regarding tenofovir alafenamide dosing intervals as a function of CKD remains warranted.

Funding

This work was supported by the Swiss HIV Cohort Study and by the Swiss National Science Foundation, grant number N° 324730_192449 (to L.A.D.).

Transparency declarations

The authors declare no conflict of interest. The funding source of the study had no role in the design of the study, data collection, data analysis, data interpretation, in writing the manuscript, or in the decision to submit the article for publication.

Supplementary data

Supplementary Methods, Figures S1 to S6, and Tables S1 to S4 are available as Supplementary data at *JAC* Online.

References

1 Benítez-Gutiérrez L, Soriano V, Requena S *et al.* Treatment and prevention of HIV infection with long-acting antiretrovirals. *Expert Rev Clin Pharmacol* 2018; **11**: 507–17. https://doi.org/10.1080/17512433.2018.1453805

2 Gibson AK, Shah BM, Nambiar PH *et al.* Tenofovir alafenamide. *Ann Pharmacother* 2016; **50**: 942–52. https://doi.org/10.1177/1060028016660812

3 Ruane PJ, DeJesus E, Berger D *et al.* Antiviral activity, safety, and pharmacokinetics/pharmacodynamics of tenofovir alafenamide as 10-day monotherapy in HIV-1-positive adults. *J Acquir Immune Defic Syndr* 2013; **63**: 449–55. https://doi.org/10.1097/QAI.0b013e3182965d45

4 Podany AT, Bares SH, Havens J *et al.* Plasma and intracellular pharmacokinetics of tenofovir in patients switched from tenofovir disoproxil fumarate to tenofovir alafenamide. *AIDS* 2018; **32**: 761–5. https://doi.org/10.1097/QAD.0000000000001744

5 Ray AS, Fordyce MW, Hitchcock MJM. Tenofovir alafenamide: a novel prodrug of tenofovir for the treatment of human immunodeficiency virus. *Antiviral Res* 2016; **125**: 63–70. https://doi.org/10.1016/j.antiviral.2015.11.009

6 Gupta SK, Post FA, Arribas JR *et al.* Renal safety of tenofovir alafenamide vs. tenofovir disoproxil fumarate: a pooled analysis of 26 clinical trials. *AIDS* 2019; **33**: 1455–65. https://doi.org/10.1097/QAD.0000000000002223

7 Cattaneo D, Minisci D, Baldelli S *et al.* Effect of cobicistat on tenofovir disoproxil fumarate (TDF): what is true for TAF may also be true for TDF.

Downloaded from https://academic.oup.com/jac/article/78/6/1433/7115733 by Université de Lausanne user on 17 January 2024

J Acquir Immune Defic Syndr 2018; **77**: 86–92. https://doi.org/10.1097/QAI.0000000000001558

8 Begley R, Das M, Zhong L *et al*. Pharmacokinetics of tenofovir alafenamide when coadministered with other HIV antiretrovirals. *J Acquir Immune Defic Syndr* 2018; **78**: 465–72. https://doi.org/10.1097/QAI.0000000000001699

9 Zack J, Chu H, Chuck S *et al*. Bioequivalence of two co-formulations of emtricitabine/tenofovir alafenamide fixed-dose combinations with 200/10 mg and 200/25 mg. *J Bioequiv Bioavailab* 2016; **8**: 1–6.

10 Wassner C, Bradley N, Lee Y. A review and clinical understanding of tenofovir: tenofovir disoproxil fumarate versus tenofovir alafenamide. *J Int Assoc Provid AIDS Care* 2020; **19**: 2325958220919231. https://doi.org/10.1177/2325958220919231

11 Wonganan P, Limpanasithikul W, Jianmongkol S *et al*. Pharmacokinetics of nucleoside/nucleotide reverse transcriptase inhibitors for the treatment and prevention of HIV infection. *Expert Opin Drug Metab Toxicol* 2020; **16**: 551–64. https://doi.org/10.1080/17425255.2020.1772755

12 European Medicines Agency (EMA). BIKTARVY film-coated tablets. Summary of the product characteristics. https://www.ema.europa.eu/en/documents/product-information/biktarvy-epar-product-information_en.pdf

13 World Health Organization. Updated recommendations on first-line and second-line antiretroviral regimens and post-exposure prophylaxis and recommendations on early infant diagnosis of HIV: interim guidelines: supplement to the 2016 consolidated guidelines on the use of antiretroviral drugs for treating and preventing HIV infection. 2018. https://apps.who.int/iris/handle/10665/277395

14 Saag MS, Gandhi RT, Hoy JF *et al*. Antiretroviral drugs for treatment and prevention of HIV infection in adults: 2020 recommendations of the International Antiviral Society-USA panel. *JAMA* 2020; **324**: 1651–69. https://doi.org/10.1001/jama.2020.17025

15 Ackaert O, McDougall D, Pérez-Ruixo C *et al*. Population pharmacokinetic analysis of darunavir and tenofovir alafenamide in HIV-1-infected patients on the darunavir/cobicistat/emtricitabine/tenofovir alafenamide single-tablet regimen (AMBER and EMERALD studies). *AAPS J* 2021; **23**: 82. https://doi.org/10.1208/s12248-021-00607-8

16 Greene SA, Chen J, Prince HMA *et al*. Population modeling highlights drug disposition differences between tenofovir alafenamide and tenofovir disoproxil fumarate in the blood and semen. *Clin Pharmacol Ther* 2019; **106**: 821–30. https://doi.org/10.1002/cpt.1464

17 Garrett KL, Chen J, Maas BM *et al*. A pharmacokinetic/pharmacodynamic model to predict effective HIV prophylaxis dosing strategies for people who inject drugs. *J Pharmacol Exp Ther* 2018; **367**: 245–51. https://doi.org/10.1124/jpet.118.251009

18 Xiao D, Ling KHJ, Custodio J *et al*. Quantitation of intracellular triphosphate metabolites of antiretroviral agents in peripheral blood mononuclear cells (PBMCs) and corresponding cell count determinations: review of current methods and challenges. *Expert Opin Drug Metab Toxicol* 2018; **14**: 781–802. https://doi.org/10.1080/17425255.2018.1500552

19 De Nicolò A, Ianniello A, Ferrara M *et al*. Validation of a UHPLC-MS/MS method to quantify twelve antiretroviral drugs within peripheral blood mononuclear cells from people living with HIV. *Pharmaceuticals (Basel)* 2021; **14**: 12.

20 Courlet P, Spaggiari D, Cavassini M *et al*. Determination of nucleosidic/tidic reverse transcriptase inhibitors in plasma and cerebrospinal fluid by ultra-high-pressure liquid chromatography coupled with tandem mass spectrometry. *Clin Mass Spectrom* 2018; **8**: 8–20. https://doi.org/10.1016/j.clinms.2018.04.001

21 Wiriyakosol N, Puangpetch A, Manosuthi W *et al*. A LC/MS/MS method for determination of tenofovir in human plasma and its application to toxicity monitoring. *J Chromatogr B Analyt Technol Biomed Life Sci* 2018; **1085**: 89–95. https://doi.org/10.1016/j.jchromb.2018.03.045

22 Courlet P, Livio F, Guidi M *et al*. Polypharmacy, drug-drug interactions, and inappropriate drugs: new challenges in the aging population with HIV. *Open Forum Infect Dis* 2019; **6**: ofz531. https://doi.org/10.1093/ofid/ofz531

23 European Medicines Agency (EMA). Summary of product characteristics. Vemlidy 25 mg film-coated tablets. https://www.ema.europa.eu/en/documents/product-information/vemlidy-epar-product-information_en.pdf

24 Lindbom L, Pihlgren P, Jonsson EN. PsN-Toolkit–a collection of computer intensive statistical methods for non-linear mixed effect modeling using NONMEM. *Comput Methods Programs Biomed* 2005; **79**: 241–57. https://doi.org/10.1016/j.cmpb.2005.04.005

25 Keizer RJ, van Benten M, Beijnen JH *et al*. Piraña and PCluster: a modeling environment and cluster infrastructure for NONMEM. *Comput Methods Programs Biomed* 2011; **101**: 72–9. https://doi.org/10.1016/j.cmpb.2010.04.018

26 Cottrell ML, Garrett KL, Prince HMA *et al*. Single-dose pharmacokinetics of tenofovir alafenamide and its active metabolite in the mucosal tissues. *J Antimicrob Chemother* 2017; **72**: 1731–40. https://doi.org/10.1093/jac/dkx064

27 Cockcroft DW, Gault MH. Prediction of creatinine clearance from serum creatinine. *Nephron* 1976; **16**: 31–41. https://doi.org/10.1159/000180580

28 Levey AS, Stevens LA, Schmid CH *et al*. A new equation to estimate glomerular filtration rate. *Ann Intern Med* 2009; **150**: 604–12. https://doi.org/10.7326/0003-4819-150-9-200905050-00006

29 U.S. Food and Drug Administration. Drug development and drug interactions | Table of substrates, inhibitors and inducers. Table 5.2: Examples of clinical inhibitors for transporters (for use in clinical DDI studies and drug labeling). https://www.fda.gov/drugs/drug-interactions-labeling/drug-development-and-drug-interactions-table-substrates-inhibitors-and-inducers#table5-2

30 UpToDate. Inhibitors and inducers of P-glycoprotein (P-gp) drug efflux pump (P-gp multidrug resistance transporter). https://www.uptodate.com/contents/image/print?imageKey=EM%2F73326&topicKey=RHE

31 Elmeliegy M, Vourvahis M, Guo C *et al*. Effect of P-glycoprotein (P-gp) inducers on exposure of P-gp substrates: review of clinical drug-drug interaction studies. *Clin Pharmacokinet* 2020; **59**: 699–714. https://doi.org/10.1007/s40262-020-00867-1

32 Service de pharmacologie et toxicologie cliniques, Hôpitaux Universitaires de Genève (HUG). Interactions médicamenteuses, cytochromes P450 et P-glycoprotéine (Pgp). https://www.hug.ch/sites/interhug/files/structures/pharmacologie_et_toxicologie_cliniques/images/carte_des_cytochromes_2020.pdf

33 Ghane Shahrbaf F, Assadi F. Drug-induced renal disorders. *J Renal Inj Prev* 2015; **4**: 57–60.

34 Goldstein SL, Kirkendall E, Nguyen H *et al*. Electronic health record identification of nephrotoxin exposure and associated acute kidney injury. *Pediatrics* 2013; **132**: e756–67. https://doi.org/10.1542/peds.2013-0794

35 Naughton CA. Drug-induced nephrotoxicity. *Am Family Phys* 2008; **78**: 743–50.

36 Ahn JE, Karlsson MO, Dunne A *et al*. Likelihood based approaches to handling data below the quantification limit using NONMEM VI. *J Pharmacokinet Pharmacodyn* 2008; **35**: 401–21. https://doi.org/10.1007/s10928-008-9094-4

37 Bonate P. *Pharmacokinetic-Pharmacodynamic Modeling and Simulation*. Springer, 2011.

Downloaded from https://academic.oup.com/jac/article/78/6/1433/7115733 by Université de Lausanne user on 17 January 2024

38 Guidi M, Csajka C, Buclin T. Parametric approaches in population pharmacokinetics. *J Clin Pharmacol* 2022; **62**: 125–41. https://doi.org/10.1002/jcph.1633

39 Duffull SB, Wright DF, Winter HR. Interpreting population pharmacokinetic-pharmacodynamic analyses – a clinical viewpoint. *Br J Clin Pharmacol* 2011; **71**: 807–14. https://doi.org/10.1111/j.1365-2125.2010.03891.x

40 Bergstrand M, Hooker AC, Wallin JE *et al*. Prediction-corrected visual predictive checks for diagnosing nonlinear mixed-effects models. *AAPS J* 2011; **13**: 143–51. https://doi.org/10.1208/s12248-011-9255-z

41 Jonsson EN, Karlsson MO. Xpose–an S-PLUS based population pharmacokinetic/pharmacodynamic model building aid for NONMEM. *Comput Methods Programs Biomed* 1999; **58**: 51–64. https://doi.org/10.1016/S0169-2607(98)00067-4

42 Sheiner LB, Beal SL. Some suggestions for measuring predictive performance. *J Pharmacokinet Biopharm* 1981; **9**: 503–12. https://doi.org/10.1007/BF01060893

43 Custodio JM, Garner W, Callebaut C. The pharmacokinetics of tenofovir and tenofovir-diphosphate following administration of tenofovir alafenamide vs tenofovir disoproxil fumarate. Abstract 6. *International Workshop on Clinical Pharmacology of HIV & Hepatitis Therapy*, Washington, DC, 2015.

44 Thurman AR, Schwartz JL, Cottrell ML *et al*. Safety and pharmacokinetics of a tenofovir alafenamide fumarate-emtricitabine based oral antiretroviral regimen for prevention of HIV acquisition in women: a randomized controlled trial. *eClinicalMedicine* 2021; **36**: 100893. https://doi.org/10.1016/j.eclinm.2021.100893

45 Yamada H, Yonemura T, Nemoto T *et al*. Pharmacokinetics of tenofovir alafenamide, tenofovir, and emtricitabine following administration of coformulated emtricitabine/tenofovir alafenamide in healthy Japanese subjects. *Clin Pharmacol Drug Dev* 2019; **8**: 511–20. https://doi.org/10.1002/cpdd.623

46 Custodio JM, Fordyce M, Garner W *et al*. Pharmacokinetics and safety of tenofovir alafenamide in HIV-uninfected subjects with severe renal impairment. *Antimicrob Agents Chemother* 2016; **60**: 5135–40. https://doi.org/10.1128/AAC.00005-16

47 Jullien V, Tréluyer JM, Rey E *et al*. Population pharmacokinetics of tenofovir in human immunodeficiency virus-infected patients taking highly active antiretroviral therapy. *Antimicrob Agents Chemother* 2005; **49**: 3361–6. https://doi.org/10.1128/AAC.49.8.3361-3366.2005

48 University of Liverpool. Antiretroviral dosing in adults with renal impairment. Revised July 2019. www.hiv-druginteractions.org/prescribing_resources/hiv-guidance-arvs-renal

49 European Medicines Agency (EMA). Summary of product characteristics. Tenofovir disoproxil Mylan 245 mg film coated tablets. https://www.ema.europa.eu/en/documents/product-information/tenofovir-disoproxil-mylan-epar-product-information_en.pdf

50 Yager JL, Brooks KM, Castillo-Mancilla JR *et al*. Tenofovir-diphosphate in peripheral blood mononuclear cells during low, medium, and high adherence to F/TAF vs. F/TDF. *AIDS* 2021; **35**: 2481–7. https://doi.org/10.1097/QAD.0000000000003062

51 Brooks KM, Castillo-Mancilla JR, Morrow M *et al*. Pharmacokinetics and renal safety of tenofovir alafenamide with boosted protease inhibitors and ledipasvir/sofosbuvir. *J Antimicrob Chemother* 2020; **75**: 3303–10. https://doi.org/10.1093/jac/dkaa299

52 Dumond JB, Greene SA, Prince H *et al*. Differential extracellular, but similar intracellular, disposition of two tenofovir formulations in the male genital tract. *Antivir Ther (Lond)* 2019; **24**: 45–50. https://doi.org/10.3851/IMP3277

53 Bazzoli C, Jullien V, Le Tiec C *et al*. Intracellular pharmacokinetics of antiretroviral drugs in HIV-infected patients, and their correlation with drug action. *Clin Pharmacokinet* 2010; **49**: 17–45. https://doi.org/10.2165/11318110-000000000-00000

54 Duwal S, Schütte C, von Kleist M. Pharmacokinetics and pharmacodynamics of the reverse transcriptase inhibitor tenofovir and prophylactic efficacy against HIV-1 infection. *PLoS One* 2012; **7**: e40382. https://doi.org/10.1371/journal.pone.0040382

Downloaded from https://academic.oup.com/jac/article/78/6/1433/7115733 by Université de Lausanne user on 17 January 2024